




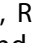

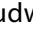






Gut microbiota composition as a candidate risk factor for dimethyl fumarate-induced lymphopenia in multiple sclerosis

Martin Diebold ^{a,b,*}, Marco Meola ^{c,d,e,f,*}, Srinithi Purushothaman ^{c,d,e,*}, Lena K Siewert ^a, Elisabeth Pössnecker ^a, Tim Roloff ^{c,d,e,f}, Raija LP Lindberg ^a, Jens Kuhle ^a, Ludwig Kappos ^a, Tobias Derfuss ^a, Adrian Egli ^{c,d,e,*}, and Anne-Katrin Pröbstel ^{a,*}

^aDepartments of Neurology, Biomedicine and Clinical Research & Research Center for Clinical Neuroimmunology and Neuroscience Basel (RC2NB), University Hospital and University of Basel, Basel, Switzerland; ^bInstitute of Neuropathology, Neurocenter, University Hospital Freiburg, University of Freiburg, Freiburg, Germany; ^cDivision of Clinical Bacteriology and Mycology, University Hospital Basel, Basel, Switzerland; ^dApplied Microbiology Research, Department of Biomedicine, University of Basel, Basel, Switzerland; ^eInstitute for Medical Microbiology, University of Zurich, Zurich, Switzerland; ^fSwiss Institute of Bioinformatics, Basel, Switzerland

ABSTRACT

Mounting evidence points towards a pivotal role of gut microbiota in multiple sclerosis (MS) pathophysiology. Yet, whether disease-modifying treatments alter microbiota composition and whether microbiota shape treatment response and side-effects remain unclear. In this prospective observational pilot study, we assessed the effect of dimethyl fumarate (DMF) on gut microbiota and on host/microbial metabolomics in a cohort of 20 MS patients. Combining state-of-the-art microbial sequencing, metabolome mass spectrometry, and computational analysis, we identified longitudinal changes in gut microbiota composition under DMF-treatment and an increase in citric acid cycle metabolites. Notably, DMF-induced lymphopenia, a clinically relevant safety concern, was correlated with distinct baseline microbiome signatures in MS patients. We identified gastrointestinal microbiota as a key therapeutic target for metabolic properties of DMF. By characterizing gut microbial composition as a candidate risk factor for DMF-induced lymphopenia, we provide novel insights into the role of microbiota in mediating clinical side-effects.

ARTICLE HISTORY

Received 25 July 2022
Revised 12 October 2022
Accepted 7 November 2022

KEYWORDS



Multiple sclerosis;
microbiome; dimethyl
fumarate; lymphopenia;
metabolomics; therapeutic
biomarker

Introduction


While studying gut microbiota is a promising approach to better understand pathophysiology and open novel therapeutic avenues in multiple sclerosis (MS), we lack fundamental knowledge about how disease-modifying therapies (DMTs) affect gut microbiota composition and metabolism. Further, it remains unclear whether distinct microbial taxa shape treatment response and drug-induced side-effects¹.

In this context, recent publications^{2–6} set a spotlight on dimethyl fumarate (DMF), a frequently administered DMT. DMF is a *bona fide* immunometabolic compound with metabolic properties on the mitochondrial respiration of activated T cells⁵ and restrictive effects on glycolysis in lymphocytes.^{2,6} Yet, it is likely that the effects of this empirically developed, untargeted, small molecule reach beyond T cells,

potentially affecting other metabolically active human and bacterial cells. Notably, DMF, a citrate cycle derivative, is rapidly metabolized within the gastrointestinal tract and causes self-limited gastrointestinal side-effects in many patients.⁷ Indeed, cross-sectional observations in MS patients indicated that DMF may affect not only immune cells but also the gastrointestinal microbiota^{8–10}, and thereby potentially reduce the release of direct neurotoxic compounds.³ However, knowledge regarding longitudinal alterations of the gut microbiota under DMF and their metabolic consequences is limited. We used the setting of an established prospective observational study,⁶ to explore the effect of DMF on the metabolic profile of the host and on the gut microbiome. Further, we addressed whether distinct microbial signatures can be linked to treatment response and DMF-induced side-effects.

CONTACT Anne-Katrin Pröbstel  anne-katrin.proebstel@usb.ch  Departments of Neurology, Biomedicine and Clinical Research & Research Center for Clinical Neuroimmunology and Neuroscience Basel (RC2NB), University Hospital and University of Basel, Basel, Switzerland

*These authors contributed equally to this work.

 Supplemental data for this article can be accessed online at <https://doi.org/10.1080/19490976.2022.2147055>

© 2022 The Author(s). Published with license by Taylor & Francis Group, LLC.

This is an Open Access article distributed under the terms of the Creative Commons Attribution License (<http://creativecommons.org/licenses/by/4.0/>), which permits unrestricted use, distribution, and reproduction in any medium, provided the original work is properly cited.

Results

We enrolled 20 patients with relapsing-remitting MS (RRMS), a mean age of 42 y (range 23–59), and marginal female preponderance (55%) (Table 1). Exploring the imprint of DMF on the host serum metabolome and gut microbial metabolome in a longitudinal setup, we assessed early changes in patients' metabolomes and microbiomes and compared them to outcomes during 12 months under DMF therapy (Figure 1a).

DMF alters host and microbiota metabolome

Assessing patient sera, a total of 805 compounds of known identity were recognized by ultrahigh-performance liquid chromatography-tandem mass spectroscopy (UPLC-MS/MS), of which 31 statistically significantly increased (n = 21) or decreased (n = 10) during the first 3 months of treatment (corrected for False Discovery Rate, $q < 0.05$). Additionally, we conducted a random forest (RF) analysis comparing baseline and three-month groups to rank these effects (Figure 1b). By both approaches, several of the top 30 biochemicals predicting group separation were linked to essential energy metabolism, specifically containing increased intermediates of the citrate cycle. The most

significant increases were identified for fumarate (2.3-fold, $q = 0.008$) and its neighboring metabolites succinate (1.5-fold, $q = 0.006$) and malate (1.3-fold, $q = 0.016$) (Figure 1c), in serum.

Next, we assessed longitudinal changes in the gut microbiome by amplicon sequencing (rarefaction curve eFigure 1a). While no significant changes in the alpha diversity (eFigure 1b) and no separate grouping in a non-metric multidimensional scaling (NMDS) representation were observed regarding DMF treatment (Figure 1d, eFigure S1c) or previous treatments (eFigure S1d), we identified significantly decreased (n = 2) and increased (n = 1) abundance of a few bacterial species under DMF treatment (Figure 1e). The group of decreased bacteria prominently included *Coproccoccus eutactus* ($P_{\text{adj}} = 0.012$), *Enterococcus gilvus* ($P_{\text{adj}} = 0.042$), and – though not significant – *Akkermansia muciniphilia* ($P_{\text{adj}} = 0.138$). *Lactobacillus pentosus* ($P_{\text{adj}} = 0.012$) was significantly increased upon treatment (Figure 1e–f, eTables S1–2). To compare the metabolic alterations on the host (patient) and the microbiota (eFigure S1e–h), we used PICRUST2 for imputing microbial metabolomics from 16S sequencing data. In the gut, 13 metabolites were identified uniquely before treatment onset and 29 metabolites only after 3 months (Figure 1g, eTable S3). Complementing the serum metabolite analysis, an increased abundance of

Table 1. Clinical data of the study cohort (baseline characteristics and outcomes of each individual of the study cohort).

Baseline characteristics								Outcomes				
Patient ID*	Age (a)	Sex	Disease course	Disease duration (a)	Previous disease activity (relapses/2a)	Previous DMT	Delay from previous DMT (d)	EDSS at baseline	Disease activity (1: MRI, 2: MRI + relapse)	Lymphopenia (<700/ μ l in first year)	GI symptoms	Flushing
1	36	m	RRMS	0.3	0	None	-	1.0	0	0	0	1
2	38	m	RRMS	0.2	2	None	-	2.0	0	0	0	0
3	45	f	RRMS	3.8	0	Daclizumab	27	2.0	0	1	0	1
4	59	f	RRMS	3.4	0	Fingolimod	104	3.5	0	1	0	0
5	54	f	RRMS	8.1	0	Glatirameracetate	12	3.0	0	0	1	1
6	43	m	RRMS	2.3	0	Teriflunomide	53	2.0	0	1	1	1
7	50	f	RRMS	11.7	0	Interferon beta	546	2.5	0	1	0	1
9	57	f	RRMS	0.9	2	None	-	3.0	0	1	0	0
10	40	f	RRMS	0.3	1	None	-	1.5	0	1	0	0
13	32	m	RRMS	0.4	1	None	-	1.0	2	0	0	0
14	23	m	RRMS	0.2	1	None	-	2.0	1	0	0	1
15	42	m	RRMS	0.2	2	None	-	3.0	0	0	1	1
16	37	f	RRMS	7.4	1	Teriflunomide	74	1.5	0	1	1	1
17	44	m	RRMS	10.2	0	Fingolimod	115	4.0	0	0	0	0
19	30	m	RRMS	0.1	2	None	-	2.0	0	0	0	0
21	49	f	RRMS	0.1	1	Glatirameracetate	16	1.5	2	1	0	0
25	34	m	RRMS	1.0	0	Glatirameracetate	17	0.0	1	0	0	0
27	27	f	RRMS	6.5	4	Teriflunomide	62	3.0	0	0	0	1
29	50	f	RRMS	10.6	0	Glatirameracetate	5	1.0	1	1	0	0
33	41	f	RRMS	0.1	1	None	-	2.5	0	0	0	0

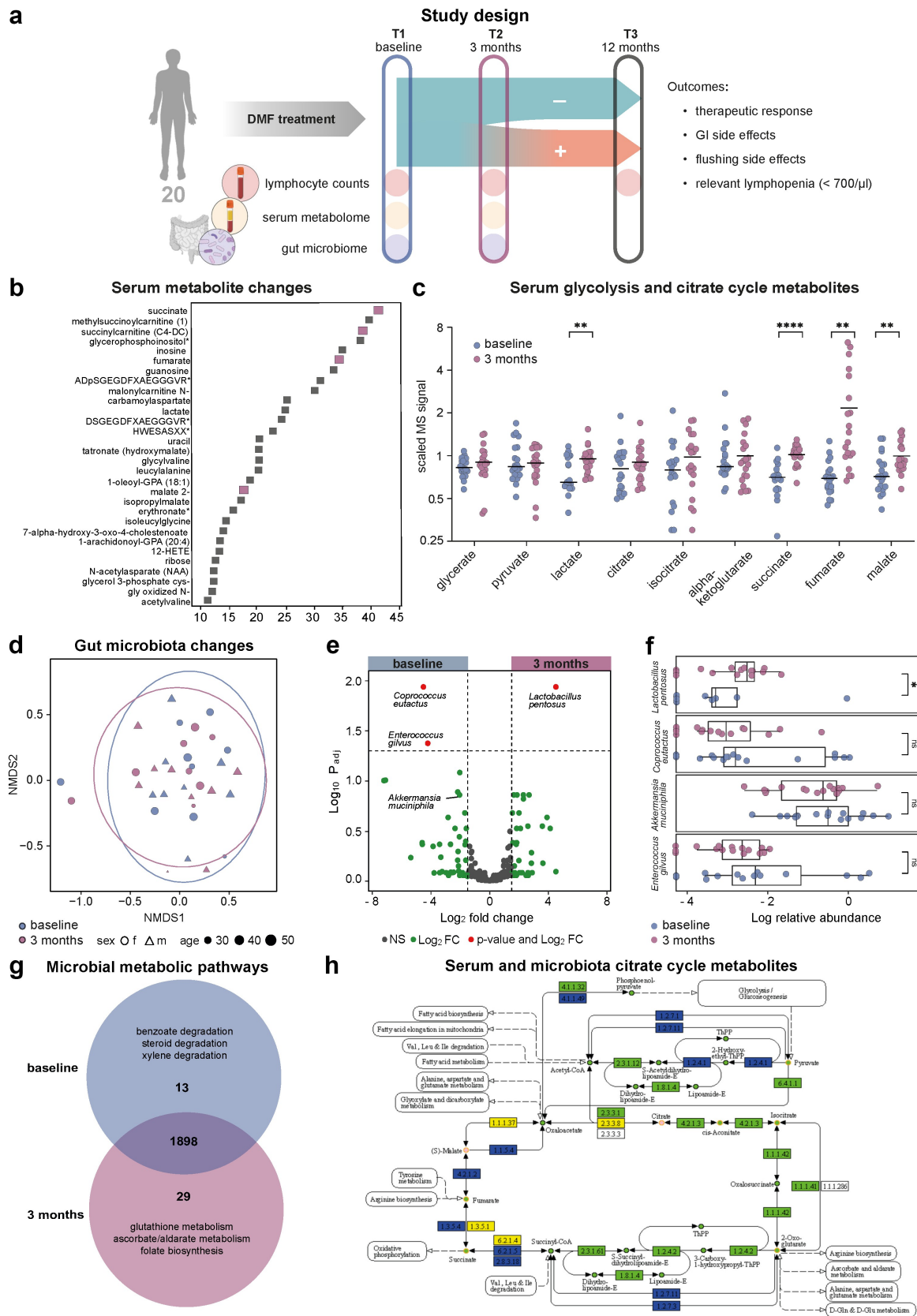


Figure 1. DMF treatment specifically recomposes the gut microbiota. (a) In this prospective observational study, serum metabolome, gastrointestinal microbiota as well as clinical and paraclinical parameters were assessed in 20 individuals during the first year of oral DMF treatment to delineate markers of clinical outcomes. (b) Random Forest analysis of longitudinal changes within all 805 identified serum metabolites. Higher mean decrease accuracy suggest more relevant longitudinal changes (top 30 metabolites

citrate cycle intermediates was observed in the microbiome profile under DMF treatment. Under treatment, we furthermore detected compound C05422, involved in antioxidative ascorbate, aldarate, and glutathione metabolism (Figure 1h).

DMF-induced lymphopenia associates with distinct baseline microbiome signatures

We next assessed correlations between clinical outcomes and microbiota composition. Notably, patients with or without subsequent treatment-associated lymphopenia clustered based on their microbiome composition (Figure 2a). By contrast, we observed no altered patterns in the NMDS representation for disease activity, gastrointestinal, or flushing side effects (eFigure S2a-c). With the exception of patient 16 (microbiota characterized by high abundances of *Streptococci*), all samples of the lymphopenia group showed a similar taxonomic pattern already at baseline. To assess this lymphopenia-associated microbiome composition, we identified the most relevant single species for development of lymphopenia (Figure 2b-c, eFigure S2d-e, metabolic features eFigure S2f-i, excluding patient 16 due to its outlier status, eTables S4–6). In two independent analyses of our dataset, we identified a group of bacteria composed of *A. muciniphila*, *Bacteroides dorei*, *Agathobacter rectale*, *Prevotella copri*, and *P. falseni* (by LEfSe Figure 2c-d, by Euclidean vector assessment of a principal component analysis Figure 2b and eFigure S2d). Notably, these species discriminated between patients with and without subsequent lymphopenia before treatment (eFigure S2e). We observed a constant presence of *A. muciniphila* and absence of *P. copri* with the occurrence of lymphopenia. Conversely, subjects with no lymphopenia were characterized by the

presence or absence of both *A. muciniphila* and *P. copri* or the absence of *A. muciniphila* in presence of *P. copri* (Figure 2e). Sensitivity and specificity of lymphopenia prediction as side effects based solely on these two species was 0.85. To determine a third species potentially increasing the discriminatory power between patients with and without subsequent lymphopenia, we tested several combinations of ternary plots composed of *A. muciniphila*, *P. copri*, and a third species candidate – such as *A. rectale* – highlighted in the previous multivariate analyses (Figure 2f and eFigure S2j).

Discussion

In this study, we aimed to assess differences in the metabolomes of patients and their microbiota related to DMF treatment and identified bidirectional treatment-microbiota associations. While the treatment *per se* influenced the microbiota composition, a specific constellation of certain commensal taxa served as a candidate predictor for the occurrence of lymphopenia under treatment.

Our findings demonstrate a specific rearrangement of MS-associated taxa¹¹ upon DMF treatment with a decrease in MS-associated proinflammatory taxa, such as *A. muciniphila* and *C. eutactus*,^{1,12,13} and an increase in allegedly beneficial, anti-inflammatory species, like *L. pentosus*,^{10,14} substantiating previous cross-sectional data.^{8–10} Detailing the metabolic properties of DMF,^{2,5,6} we demonstrated increasing late citrate cycle intermediates not only in the host's serum (where they had previously been hypothesized) but also in the microbial metabolism. Whereas these beneficial immunomodulatory effects in two compartments may be explained by simultaneous metabolic changes in bacteria and blood under DMF, an alternative interpretation would identify the changing

shown), citrate cycle metabolites are marked in purple. (c) Glycolysis and citrate cycle metabolites, as measured by mass spectrometry, compared between baseline and 3 months timepoints. (d) Non-metric multidimensional representation (NMDS) of the gastrointestinal microbiota composition of baseline (blue) and 3 months (purple) samples (stress: 0.17). Circles represent confidence interval of 95%. (e) Volcano plot of 3 months/baseline microbial species, significantly ($p_{adj} < 0.05$) overrepresented species at baseline (left) or 3 months (right) illustrated in red. (f) Box plots of log₁₀-transformed normalized relative abundances of the four most affected (according to volcano plot, 1E) microbial species at baseline (blue) and 3 months (purple). (g) Venn diagram from AMON analysis for baseline vs. 3 months for metabolic pathways of the gastrointestinal microbiota. (h) Visualization of AMON analysis of putative origin of metabolites (circles) and enzymatic reactions (rectangles) of the citrate cycle, with dark blue indicating exclusive bacterial origin, yellow indicating exclusive human origin, and orange indicating compounds detected in serum. Green color labels compounds of either human or bacterial origin without certain attribution.

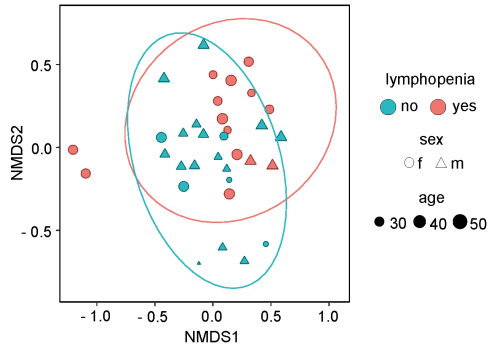
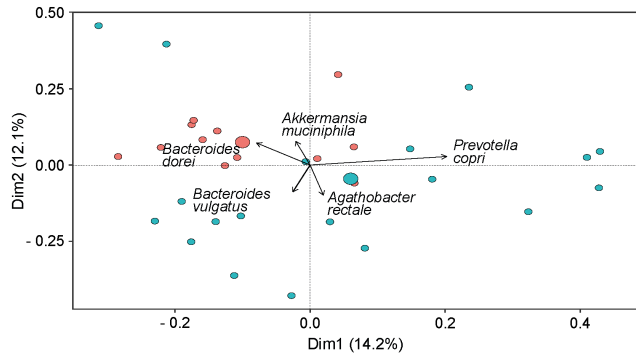
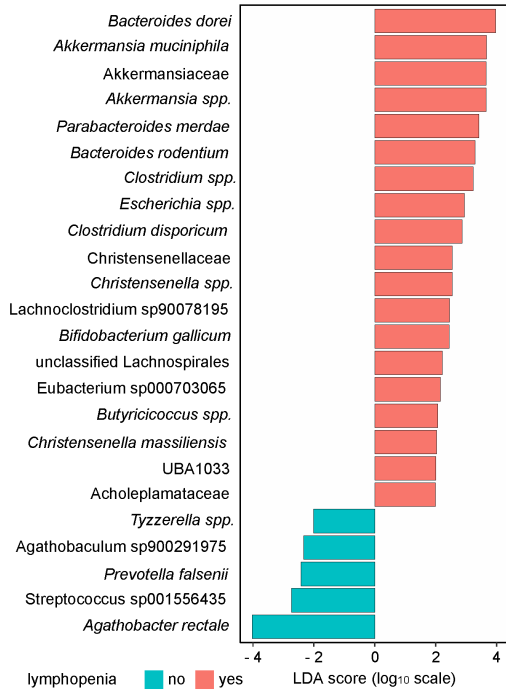
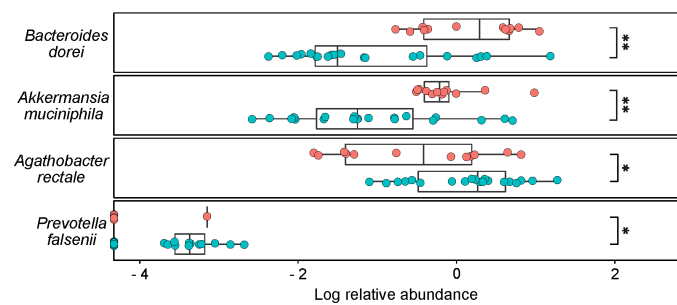
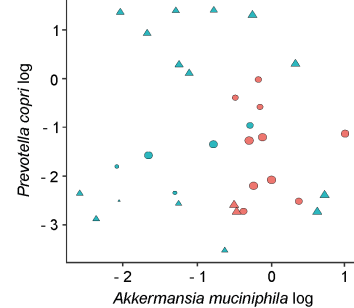
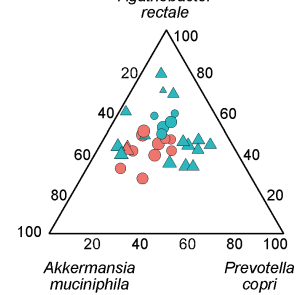
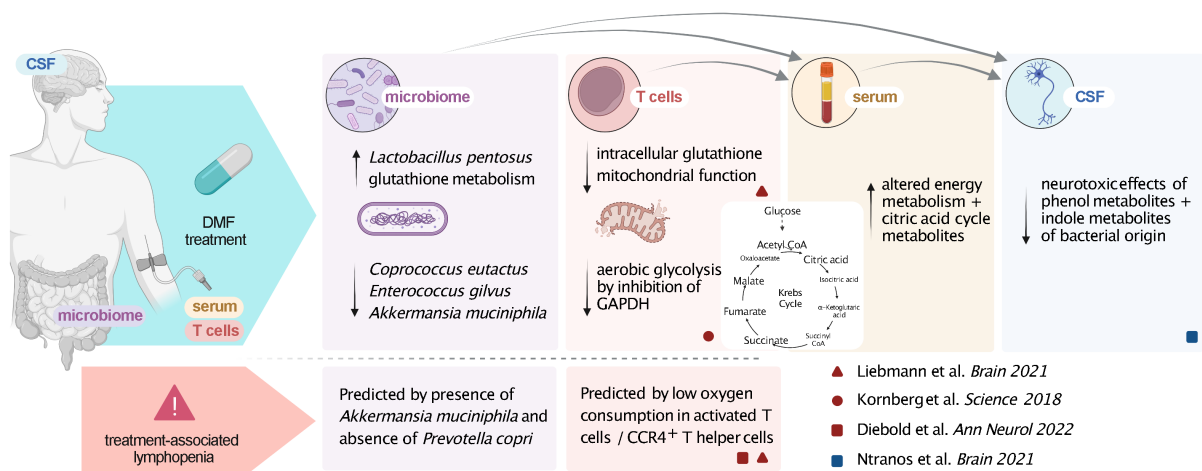
a Microbiota composition in +/- lymphopenia**b****c****d****e****f****g** Immunometabolic properties of DMF reach beyond immune cells

Figure 2. Microbiota composition predisposes to DMF-associated lymphopenia. (a) Non-metric multidimensional representation (NMDS) of the gastrointestinal microbiota composition of samples from individuals with (red) or without (turquoise) subsequent DMF-associated lymphopenia. Circles represent confidence interval of 95% (stress: 0.17). (b) Principal component analysis of the gastrointestinal microbiota composition of samples from individuals with (red) or without (turquoise) subsequent DMF-associated

gastrointestinal microbiota composition as the reason for a cascade of effects, including lymphocyte alterations and a loss of neurotoxic bacterial metabolites observed in the serum and cerebrospinal fluid of patients³ (Figure 2g). The latter hypothesis may be supported by the short half-life of fumaric acid esters with rapid degradation in the citrate cycle. The gut microbiota are therefore privileged over circulating immune cells by their early, metabolically relevant contact with DMF. In light of the very limited understanding of the direct effects of fumaric acid esters on specific bacteria,^{15,16} further research will be needed to dissect metabolic properties of DMF on microbiota – and their effects on host immune cells.

Further, our observation that baseline microbiota composition may be a critical mediator of lymphopenia, as a side effect of DMF, suggests that the drug-microbiome interplay reaches beyond these therapeutic effects. Lymphopenia represents the main safety concern of DMF treatment due to its association with rare cases of progressive multifocal leukoencephalopathy.¹⁷ While it is known that patients with relevant lymphopenia are older and have lower baseline lymphocyte counts – specifically of CCR4⁺ T helper cells –^{4,18} more refined biomarkers for risk stratification of this severe side effect are utmost needed to tailor personalized treatment recommendations. Notably, we here observed an association between the baseline presence of *A. muciniphila* and absence of *P. copri* with the development of lymphopenia during treatment. In turn, lymphopenia was absent in patients with simultaneous appearance of both *A. muciniphila* and *P. copri*, indicating a possible counteracting effect by the presence of *P. copri*. Of interest, these taxa were previously described in association with MS and other autoimmune disorders. Namely, *A. muciniphila* and *B. dorei*^{1,19} – both overrepresented in lymphopenia patients – and *P. copri* were

shown to be reduced in MS patients¹² but increase upon DMT.¹¹ While we cannot exclude that this small exploratory pilot study may have been affected by unrecorded dietary effects or under-powered to identify associations for rare events – including an association of gut microbiota with disease activity²⁰ – observations from this first longitudinal microbiome analysis under DMF provide pivotal evidence for a role of microbiota in the development of lymphopenia. We therefore believe that larger studies are warranted to evaluate the feasibility of microbiome testing for the prediction of DMF-associated lymphopenia in MS patients with implications for the assessment of microbiota in mediating clinically relevant side-effects under other DMTs.

Patients and methods

We prospectively collected stool and blood samples from 20 patients with RRMS intending to start DMF treatment, as an extension of the project previously published by Diebold et al. in 2018.⁶ Sampling for assessment of microbiome or metabolome predictors was scheduled at two early time-points: before first intake (baseline) and after 3 months of DMF treatment. Stool samples were collected using fecal collection kits (Epitope Diagnostics Inc., San Diego, CA) and stored at –80°C until further processing.

To cover a longer clinical and immunological follow-up, additional blood samples were collected after 12 months of DMF treatment. Blood samples from all three time points were assessed by automated flow cytometry for lymphocyte counts and major lymphocyte subpopulations (eTable 6). Detailed clinical information including survey of anamnestic and laboratory adverse events was collected at each time point. Assessed outcomes comprised adverse events (flushing and gastrointestinal side effects, relevant lymphopenia (<700/ μ l)) and

lymphopenia with Euclidean vectors representing the effects of main microbiota, excluding one individual with dominant streptococcal effect (b–f). (c) LEfSe analysis of dominant gastrointestinal microbiota of individuals with (right) and without (left) subsequent DMF-associated lymphopenia. Colored bars indicate taxa highlighted in adjunct figures. (d) Box plots of log₁₀-transformed normalized relative abundances of four most affected (according to principal component analysis, 2B, and LEfSe analysis, 2C) microbial species in samples with (red) or without (turquoise) subsequent DMF-associated lymphopenia. (e) Bi-axial dot plot of log₁₀-transformed relative abundances of *Akkermansia muciniphila* and *Prevotella copri*, color code indicating samples with (red) or without (turquoise) subsequent DMF-associated lymphopenia. (f) Ternary dot plot of the log₁₀-transformed and subsequently normalized abundances of *A. muciniphila*, *Agathobacter rectale*, and *P. copri* only, color code indicating samples with (red) or without (turquoise) subsequent DMF-associated lymphopenia. (g) Graphical summary of findings from this study and the recent literature.

disease activity (as judged by clinical relapse and MRI activity) within the first 12 months of treatment. Disease activity was assessed by recording clinical relapses and/or new lesions in T2-weighted cerebral magnetic resonance imaging (MRI) within 12 months after treatment started (Figure 1a). All participants gave written consent before enrollment. The study was conducted as a nested project within the Swiss Multiple Sclerosis Cohort Study and approved by the Ethics Committee for Northwest and Central Switzerland (EKNZ 201448/12).

Serum metabolomics

Serum samples from the first 14 patients (available at the time point of analysis) within this cohort were characterized for metabolomics by UPLC-MS/MS, as described in.⁶ Each sample was analyzed using acidic positive ion conditions, basic negative ion optimized conditions, and negative ionization. Blinded data were processed and normalized by Metabolon Inc. (Durham, USA) for all assessed samples as described previously.⁶ Results were verified by paired analysis (for time points T1 and T2) for each observation and assessed using RF analysis on all measured metabolites.

Amplicon sequencing

Stool samples of all 20 patients were assessed for their gut microbiome composition using the QIAseq 16S/ITS screening panel (QIAGEN), sequenced on a MiSeq (Illumina). In short, samples were thawed and total DNA (totDNA) from 250 mg stool was extracted with a QIAamp PowerFecal Pro DNA Kit (QIAGEN). Sequencing libraries were generated with the QIAseq 16S/ITS Screening Panels kit. For each sample, 1 ng of totDNA was amplified with each of the three Screening Panel Pools and subsequently combined and indexed. The indexed libraries were pooled equimolarly, and 15pM were loaded and sequenced PE 276 on a MiSeq v3 600-cycle kit (Illumina).

Bioinformatic & statistical analysis

The bioinformatic analysis was performed on R (R core team) using the phyloseq package (v.1.38.0).²¹

Operational taxonomic unit (OTU) abundances were calculated in the CLC microbiome analysis tool. Taxonomic annotation of the OTU reference sequences was done with the GTDB R89 database with full 16S²² and IDTAXA algorithm²³ with the DECIPHER package (v.2.22.0) in R (v4.1.2) (R Core Team 2020).

The obtained OTU abundance table, OTU reference sequences, taxonomic annotation, and metadata were imported into a phyloseq object for downstream statistical analyses with the phyloseq package (v.1.38.0)²¹ in R. Samples counts varied between 196166 and 846999 with a median count value of 359300. Out of the 8667 OTUs obtained after the bioinformatic analysis, 3176 were removed as singletons and present in <1% of the samples representing 0.073% of the overall abundances. A total of 5491 OTUs were used for downstream analyses representing 29 phyla, 55 classes, 119 orders, 194 families, 429 genera, and 914 species. All samples reached sufficient sequencing depth according to the rarefaction curve based on the detected species.

Alpha diversity indices based on species composition (richness, Shannon, Simpson, inverse Simpson, and chao1) were assessed using the phyloseq package in R. NMDS was analyzed in R with the phyloseq package using compositional species table and Bray-Curtis algorithm. Principal component analysis (PCA) plots with contribution arrows as explanatory variables were calculated in R with the factoextra package (v.1.0.7) using Hellinger transformed compositional data of species composition. The Euclidean vectors were calculated using the function `prcomp()` of the package “stat” and `fviz_pca_biplot()` of the package “factoextra.” PCA with imputed metabolic compounds from PICRUSt2 was performed on Hellinger transformed abundance data.

Differential expression analysis of the bacterial species in baseline vs. 3 months and lymphopenia vs. no lymphopenia was performed with DESeq2 package (v.1.34.0)²⁴ in R. Deseq function was run on a matrix not normalized species compositional data from phyloseq with the parameter `test = “Wald”` and `fitType = “parametric”`.

Boxplots were analyzed on normalized and log10 transformed relative abundance data of species composition. Samples were compared based on time point (baseline vs. 3 months) and side effect

(no-lymphopenia vs. lymphopenia). Significance was assessed with the `compare_mean` function of the `ggpubr` package in R using `method = "wilcox.test"` and `p.adjust.method = "hochberg"`.

Ternary plots were generated using the `ggtern` package (v.3.3.5) in R. Species count abundance data were log10 transformed and the values of the three selected species normalized. The samples were plotted according to the ratio of the log10 abundance data of the three selected species.

Functional annotation for the microbiome was performed using PICRUSt2.²⁵ The biom table was given as input to PICRUSt2. The entire pipeline was launched using `PICRUSt2_pipeline.py` command with default parameters.

Relative abundance OTU table and predicted pathway abundance tables are used as input for the LefSe analysis. The OTUs and pathways that differ significantly between the time point groups were inferred from the analysis (<http://huttenhower.sph.harvard.edu/galaxy>) with default settings. The default cut-off score of 2 was used for logarithmic LDA score.

AMON was used to predict the origin of metabolites from host (human) and microbiome.²⁶ Host metabolites with KEGG ids detected from the LC/MS and KEGG Orthologs, which are predicted for the microbiome from PICRUSt2, were given as input to AMON along with the complete flat files (reaction, ko, compound, and pathways) obtained from KEGG FTP (Academic license).^{27–30} AMON analysis is carried out for the baseline and treatment groups separately. Venn diagram method (Jvenn <http://jvenn.toulouse.inra.fr/app/example.html>) was used to identify metabolites, which were unique to the microbiome at baseline and 3 months under treatment.

Acknowledgement

We thank Diana Albertos Torres for technical support with DNA extraction, library preparation, and 16S sequencing.

Disclosure statement








M.D. received speaker honoraria from Biogen Switzerland, which were used exclusively for research purposes. R.L.P.L. has received research support from the Swiss MS Society, Swiss National Science Foundation (Grants 310030_149966), European FP6 and IMI JU programs, Roche Postdoc

Fellowship Program (RPF-program), unrestricted research grants from Novartis and Biogen. J.K. received speaker fees, research support, travel support, and/or served on advisory boards by ECTRIMS, Swiss MS Society, Swiss National Research Foundation (320030_160221), University of Basel, Bayer, Biogen, Genzyme, Merck, Novartis, Protagen AG, Roche, and Teva. 's institution (University Hospital Basel) has received steering committee, advisory board, and consultancy fees used exclusively for research support in the department, as well as support of educational activities, from Actelion, Allergan, Almirall, Baxalta, Bayer, Biogen, Celgene/Receptos, CSL Behring, Desitin, Eisai, EXCEMED, F. Hoffmann-La Roche, Genzyme, Japan Tobacco, Merck, Minorix Therapeutics, Novartis, Pfizer, Sanofi Aventis, Santhera Pharmaceuticals, and Teva Pharmaceuticals, and license fees for Neurostatus-UHB products. Research at the MS Center in Basel has been supported by grants from Bayer, Biogen, the European Union, Inno-Suisse, Novartis, the Swiss MS Society, the Swiss National Research Foundation, and Roche research foundations. T. D. received financial compensation for participation in advisory boards, steering committees, and data safety monitoring boards, and for consultation with Novartis Pharmaceuticals, Merck, Biogen, Celgene, GeNeuro, Mitsubishi Tanabe Pharma, MedDay, Roche, and Sanofi Genzyme. T.D. also received research support from Novartis, Biogen, the National Swiss Science Foundation, the European Union, and the Swiss MS Society. A.-K.P. received financial compensation for participation in advisory boards, and for consultations from Biogen and Roche, all used for research support. All other authors report no potential conflicts of interest related to this study.

Funding

This study was conducted as an investigator-initiated trial with funding from Biogen Switzerland, which had no influence on the manuscript. The study was further funded by the Swiss National Science Foundation [PCEFP3_194609], the National MS Society [FG-1708-28871], the Propatient Foundation, the Goldschmidt Jacobson Foundation, and the Gottfried and Julia Bangerter Rhyner Foundation (to A.-K.P.). Ad-personam funding for M.D. was received from the Swiss National Science Foundation [project-number 199310], the German Research Foundation [IMM-PACT-Program, 413517907] and the Julia Bangerter Rhyner Foundation.

ORCID

Martin Diebold  <http://orcid.org/0000-0001-9636-6936>
 Marco Meola  <http://orcid.org/0000-0002-8951-1514>
 Lena K Siewert  <http://orcid.org/0000-0003-3808-3377>
 Elisabeth Pössnecker  <http://orcid.org/0000-0002-6271-2404>
 Raija LP Lindberg  <http://orcid.org/0000-0003-3349-314X>
 Ludwig Kappos  <http://orcid.org/0000-0003-4175-5509>
 Tobias Derfuss  <http://orcid.org/0000-0001-8431-8769>

Adrian Egli  <http://orcid.org/0000-0002-3564-8603>
 Anne-Katrin Pröbstel  <http://orcid.org/0000-0002-7748-1872>

Data availability statement

Data will be made available in the EMBL-EBI repository [accession ID: PRJEB55040] upon publication of the manuscript.

References

1. Probstel AK, Baranzini SE. The role of the gut microbiome in multiple sclerosis risk and progression: towards characterization of the “MS microbiome. *Neurotherapeutics* [Internet] 2018; 15:126–134. Available from <http://www.ncbi.nlm.nih.gov/pubmed/29147991>
2. Kornberg MD, Bhargava P, Kim PM, Putluri V, Snowman AM, Putluri N, Calabresi PA, Snyder SH. Dimethyl fumarate targets GAPDH and aerobic glycolysis to modulate immunity. *Science* (80-) [Internet] 2018; 360:449–453. Available from <http://www.ncbi.nlm.nih.gov/pubmed/29599194>
3. Ntranos A, Park HJ, Wentling M, Tolstikov V, Amatruda M, Inbar B, Kim-Schulze S, Frazier C, Button J, Kiebish MA, et al. Bacterial neurotoxic metabolites in multiple sclerosis cerebrospinal fluid and plasma. *Brain*. 2022;145:569–583. doi:10.1093/brain/awab320.
4. Diebold M, Galli E, Kopf A, Sanderson N, Callegari I, Ingelfinger F, Núñez NG, Benkert P, Kappos L, Kuhle J, et al. Immunological predictors of dimethyl fumarate-induced lymphopenia. *Ann Neurol*. 2022;91:676–681. Epub ahead. doi:10.1002/ana.26328.
5. Liebmann M, Korn L, Janoschka C, Albrecht S, Lauks S, Herrmann AM, Schulte-Mecklenbeck A, Schwab N, Schneider-Hohendorf T, Eveslage M, et al. Dimethyl fumarate treatment restrains the antioxidative capacity of T cells to control autoimmunity. *Brain*. 2021;144:3126–3141. doi:10.1093/brain/awab307.
6. Diebold M, Sievers C, Bantug G, Sanderson N, Kappos L, Kuhle J, Lindberg RLP, Derfuss T. Dimethyl fumarate influences innate and adaptive immunity in multiple sclerosis. *J Autoimmun*. 2018;86:39–50. doi:10.1016/j.jaut.2017.09.009.
7. Kappos L, Giovannoni G, Gold R, Phillips JT, Arnold DL, Hotermans C, Zhang A, Vigiotta V, Fox RJ. Time course of clinical and neuroradiological effects of delayed-release dimethyl fumarate in multiple sclerosis. *Eur J Neurol*. 2015;22(4):664–71. doi:10.1111/ene.12624.
8. Storm-Larsen C, Myhr KM, Farbu E, Midgard R, Nyquist K, Broch L, Berg-Hansen P, Buness A, Holm K, Ueland T, et al. Gut microbiota composition during a 12-week intervention with delayed-release dimethyl fumarate in multiple sclerosis – a pilot trial. *Mult Scler J - Exp Transl Clin*. 2019;5. doi:10.1177/2055217319888767
9. Katz Sand I, Zhu Y, Ntranos A, Clemente JC, Cekanaviciute E, Brandstadter R, Crabtree-Hartman E, Singh S, Bencosme Y, Debelius J, et al. Disease-modifying therapies alter gut microbial composition in MS. *Neurol Neuroimmunol Neuroinflamm*. [Internet] 2019; 6:e517. Available from. <http://www.ncbi.nlm.nih.gov/pubmed/30568995>
10. Ma N, Wu Y, Xie F, Du K, Wang Y, Shi L, Ji L, Liu T, Ma X. Dimethyl fumarate reduces the risk of mycotoxins via improving intestinal barrier and microbiota. *Oncotarget*. 2017;8(27):44625–44638. doi:10.18632/oncotarget.17886.
11. Jangi S, Gandhi R, Cox LM, Li N, Von Glehn F, Yan R, Patel B, Mazzola MA, Liu S, Glanz BL, et al. Alterations of the human gut microbiome in multiple sclerosis. *Nat Commun*. 2016;7. doi:10.1038/ncomms12015
12. Miyake S, Kim S, Suda W, Oshima K, Nakamura M, Matsuoka T, Chihara N, Tomita A, Sato W, Kim SW, et al. Dysbiosis in the gut microbiota of patients with multiple sclerosis, with a striking depletion of species belonging to clostridia XIVa and IV clusters. *PLoS One*. 2015;10(9):e0137429. doi:10.1371/journal.pone.0137429.
13. Cantarel BL, Waubant E, Chehoud C, Kuczynski J, Desantis TZ, Warrington J, Venkatesan A, Fraser CM, Mowry EM. Gut microbiota in multiple sclerosis: possible influence of immunomodulators. *J Investig Med*. 2015;63(5):729–734. doi:10.1097/JIM.000000000000192.
14. Kim JE, Sharma A, Sharma G, Lee SY, Shin HS, Rudra D, Im SH. *Lactobacillus pentosus* modulates immune response by inducing IL-10 producing Tr1 cells. *Immune Netw*. 2019;19. doi:10.4110/in.2019.19.e39.
15. Glenn SM, Turapov O, Makarov V, Kell DB, Mukamolova GV. Dimethyl fumarate eliminates differentially culturable *Mycobacterium tuberculosis* in an intranasal murine model of tuberculosis. *Front Cell Infect Microbiol*. 2022;12:1–7. doi:10.3389/fcimb.2022.957287.
16. Van Kuijk BLM, Schlösse ES, Stams AJM. Investigation of the fumarate metabolism of the syntrophic propionate-oxidizing bacterium strain MPOB. *Arch Microbiol*. 1998;169:346–352. doi:10.1007/s002030050581.
17. Berger JR. Classifying PML risk with disease modifying therapies. *Mult Scler Relat Disord* [Internet] 2017; 12:59–63. Available from <http://www.ncbi.nlm.nih.gov/pubmed/28283109>
18. Lucchini M, Prosperini L, Buscarinu MC, Centonze D, Conte A, Cortese A, Elia G, Fantozzi R, Ferraro E, Gasperini C, et al. Predictors of lymphocyte count recovery after dimethyl fumarate-induced lymphopenia in people with multiple sclerosis. *J Neurol*. 2021;268(6):2238–2245. doi:10.1007/s00415-021-10412-0.
19. Davis-Richardson AG, Ardisson AN, Dias R, Simell V, Leonard MT, Kempainen KM, Drew JC, Schatz D, Atkinson MA, Kolaczowski B, et al. *Bacteroides dorei*

- dominates gut microbiome prior to autoimmunity in Finnish children at high risk for type 1 diabetes. *Front Microbiol.* 2014;5. doi:10.3389/fmicb.2014.00678
20. Diebold M, Galli E, Kopf A, Sanderson NSR, Callegari I, Benkert P, Nuñez NG, Ingelfinger F, Herms S, Cichon S, et al. High-dimensional immune profiling identifies a biomarker to monitor dimethyl fumarate response in multiple sclerosis. *Proc Natl Acad Sci U S A.* 2022;119:1–10. doi:10.1073/pnas.2205042119.
 21. McMurdie PJ, Holmes S. Phyloseq: an R package for reproducible interactive analysis and graphics of microbiome census data. *PLoS One.* 2013;8:e61217. doi:10.1371/journal.pone.0061217.
 22. Parks DH, Chuvochina M, Chaumeil PA, Rinke C, Mussig AJ, Hugenholtz P. A complete domain-to-species taxonomy for bacteria and archaea. *Nat Biotechnol.* 2020;38(9):1079–1086. doi:10.1038/s41587-020-0501-8.
 23. Murali A, Bhargava A, Wright ES. IDTAXA: a novel approach for accurate taxonomic classification of microbiome sequences. *Microbiome.* 2018;6. doi:10.1186/s40168-018-0521-5.
 24. Love MI, Huber W, Anders S. Moderated estimation of fold change and dispersion for RNA-seq data with DESeq2. *Genome Biol.* 2014;15(12). doi:10.1186/s13059-014-0550-8.
 25. Douglas GM, Maffei VJ, Zaneveld JR, Yurgel SN, Brown JR, Taylor CM, Huttenhower C, Langille MGI. PICRUSt2 for prediction of metagenome functions. *Nat. Biotechnol.* 2020;38(6):685–688. doi:10.1038/s41587-020-0548-6.
 26. Shaffer M, Thurimella K, Quinn K, Doenges K, Zhang X, Bokatzian S, Reisdorph N, Lozupone CA. AMON: annotation of metabolite origins via networks to integrate microbiome and metabolome data. *BMC Bioinformatics.* 2019;20. doi:10.1186/s12859-019-3176-8.
 27. Kanehisa M, Goto S, Sato Y, Kawashima M, Furumichi M, Tanabe M. Data, information, knowledge and principle: back to metabolism in KEGG. *Nucleic Acids Res [Internet]* 2014; 42:D199–205. Available from <http://www.ncbi.nlm.nih.gov/pubmed/24214961>
 28. Kanehisa M, Goto S. KEGG: Kyoto encyclopedia of genes and genomes. *Nucleic Acids Res.* 2000;28(1):27–30. doi:10.1093/nar/28.1.27.
 29. Kanehisa M. Toward understanding the origin and evolution of cellular organisms. *Protein Sci.* 2019;28(11):1947–1951. doi:10.1002/pro.3715.
 30. Kanehisa M, Furumichi M, Sato Y, Ishiguro-Watanabe M, Tanabe M. KEGG: integrating viruses and cellular organisms. *Nucleic Acids Res.* 2021;49:D545–D551. doi:10.1093/nar/gkaa970.